

# Motor Characteristics in the Control of a Compliant Load

E.G. Harokopos\* and R.W. Mayne†  
State University of New York at Buffalo, Buffalo, New York

This paper considers a servomechanism consisting of a DC-motor, a gear train and an inertial mass controlled through a compliant drive. The compliance is modeled as a spring between the gear box and inertia, and the interaction between the actuator and its load is considered. Dimensionless parameters are defined to describe this interaction, and the influence of the parameters on open- and closed-loop performance is discussed. System behavior is relatively sensitive to one particular dimensionless parameter related to damping provided by electromechanical interaction. Results of this effort illustrate the concept of quantitative controllability and indicate the possibility of controlling flexible loads conveniently by an appropriate choice of actuator parameters.

## Introduction

**A** MOST common type of servomechanism consists of a DC motor, a gear box and an essentially inertial load which is to be positioned. The key to the operation of such servomechanisms in many practical cases is the development of an effective speed control loop which is then supervised by an outer loop to control load position. Such servomechanisms have become popular because of their availability in a wide range of power levels and the flexibility offered by a computer based outer loop.

Structural flexibility exists in all servomechanisms, and, as the load to be positioned becomes more massive or more distant, low and lightly damped natural frequencies can result. These may limit the ability of the servo to provide smooth transient response at a desired speed of operation. Applications where such difficulties exist include robotics,<sup>1,2</sup> satellite tracking systems,<sup>3</sup> and flexible drive systems.<sup>4</sup> There has been considerable effort to develop control concepts to allow high speed operation of flexible systems. However, the role of the actuator and cases where interacting actuator dynamics may be significant have received little attention.<sup>5-8</sup>

The work presented here focuses on the system model of Fig. 1 where the armature voltage is the input to the open-loop system, and the rotational speed of the inertial load  $J$  is the output. The torsional spring stiffness  $K$  represents the flexibility of the rotational system. With appropriate transformations, the model can also be used to represent linear motion systems containing a cable drive or rack and pinion, for example. This effort is an outgrowth of an earlier work by Wagle<sup>9</sup> in the frequency domain where it was noted that resonant peaks in the frequency response of the system in Fig. 1 could be considerably dampened by the appropriate choice of actuator parameters. This present work focuses on the time domain and extends the open-loop conclusions into closed-loop performance via optimal control concepts and the use of Friedland's "controllability index."<sup>10</sup>

## The Motor-Load Model

In the arrangement shown in Fig. 1, the parameters  $R$ ,  $L$ ,  $B_e$ ,  $J_e$ ,  $K_m$  and  $K_g$  represent motor resistance, inductance, viscous friction, the torque constant and generator constant, respectively. The gear ratio  $n$  is the number of pinion teeth divided by the number of gear teeth, while  $K$ ,  $J$  and  $B$  are the drive stiffness, load inertia and load viscous friction. The motor input voltage, motor current and motor angular position are indicated by  $u$ ,  $i$  and  $\theta_m$ , respectively. The spring torque is  $T$ , and the load position is  $\theta_L$ . The system state equations are

$$\dot{x} = Fx + Gu \quad (1)$$

where

$$F = \begin{bmatrix} -R/L & -K_g/L & 0 & 0 \\ K_m/J_e & -B_e/J_e & -n/J_e & 0 \\ 0 & nK & 0 & -K \\ 0 & 0 & 1/J & -B/J \end{bmatrix} \quad (2)$$

$$G = [1/L \ 0 \ 0 \ 0]^T \quad (3)$$

$$x = [x_1 \ x_2 \ x_3 \ x_4]^T$$

and

$$x_1 = i, \quad x_2 = \dot{\theta}_m, \quad x_3 = T, \quad x_4 = \dot{\theta}_L$$

These state equations have been nondimensionalized by considering the magnitude and time scaling matrices  $P$  and  $P_1$  so that

$$\dot{X}^* = \frac{dX}{d\tau} = \bar{F}X + \bar{G}U \quad (4)$$

where

$$\bar{F} = P_1 P F P^{-1}, \quad \bar{G} = P_1 P G,$$

$\tau$  is dimensionless time and  $X$  is the nondimensional state vector. We define the dimensionless time with respect to the load natural frequency so that  $\tau = \sqrt{K/J}$

and

$$P_1 = \text{diag} [\sqrt{J/K} \ \sqrt{J/K} \ \sqrt{J/K} \ \sqrt{J/K}] \quad (5)$$

Also, let

$$P = \text{diag} \left[ \frac{L}{K_g} \ \sqrt{J/K} \ \frac{1}{nK} \ \frac{1}{n} \sqrt{J/K} \right] \quad (6)$$

Received April 28, 1985; revision received Sept. 3, 1985. Copyright © American Institute of Aeronautics and Astronautics, Inc., 1985. All rights reserved.

\*Graduate Student, Department of Mechanical and Aerospace Engineering; presently with AT&T Engineering Research Center, Princeton, NJ.

†Professor, Department of Mechanical and Aerospace Engineering.

These yield

$$\bar{F} = \begin{bmatrix} -C_e & -1 & 0 & 0 \\ C_e R_d J_r & -C_m & -J_r & 0 \\ 0 & 1 & 0 & -1 \\ 0 & 0 & 1 & -C_d \end{bmatrix} \quad (7)$$

and

$$\bar{G} = [1 \ 0 \ 0 \ 0]^T \quad (8)$$

with the dimensionless quantities

$$X_1 = \frac{L}{K_g} i, \quad X_2 = \frac{\dot{\theta}_m}{\sqrt{K/J}}, \quad X_3 = \frac{T}{nK}, \quad X_4 = \frac{\dot{\theta}_L}{n\sqrt{K/J}}$$

$$C_e = \frac{R/L}{\sqrt{K/J}}, \quad C_m = \frac{B_e/J_e}{\sqrt{K/J}}, \quad C_d = \frac{B/J}{\sqrt{K/J}}$$

$$R_d = \frac{K_m K_g}{n^2 R J \sqrt{K/J}}, \quad J_r = \frac{n^2 J}{J_e}, \quad U = \frac{u}{K_g \sqrt{K/J}}$$

There are five parameters which describe the nature of the motor-load system. The ratio of the motor's electrical corner frequency to the load natural frequency is given by  $C_e$ , and the motor's mechanical corner frequency relative to the load natural frequency is  $C_m$ . The parameter  $C_d$  is directly related to the damping ratio of the load, and the ratio of the load inertia (after the reduction gears) to the motor inertia is given by  $J_r$ . The fifth parameter  $R_d$  defines the electromechanical interaction between the load and the motor, and its value depends heavily on the motor parameters.

### Open Loop Behavior

In performing open loop studies of this motor-load system a wide range of parameter values were considered in Refs. 9 and 11. Those references should be consulted for further details while only the basic nature of the motor-load behavior will be discussed here. In a motor system where the flexibility of the drive is a primary concern, the natural frequency of the drive spring and load inertia will be low and will tend to dominate the dynamic response. It will be a challenge to obtain a system transient response faster than that corresponding to the load natural frequency. From this viewpoint, typical values of the dimensionless parameters  $C_e$  and  $C_m$  would inherently tend to be quite high with the motor electrical corner frequency and the motor mechanical corner frequency well above the load natural frequency. In the results to be presented,  $C_e = 10$  and  $C_m = 10$  have been emphasized. For values of  $C_e$  and  $C_m$  larger than these, the transient behavior is only slightly modified. Values of  $C_e$  and  $C_m$  less than unity indicate an actuator which is slower than the load and would not normally be expected in systems where flexibility is prominent. The value of  $C_d$  describes the load damping, and, although this may be difficult to define exactly in practice, only small values of  $C_d$  are of interest with oscillatory loads. A value of  $C_d = 0.02$  has been used here to depict a lightly damped condition.

Figure 2 presents a set of transient response results for  $C_e = 10$ ,  $C_m = 10$ ,  $C_d = 0.02$ ,  $J_r = 10$  and various values of  $R_d$ . Each of the load speed transients shown has been normalized by its steady-state gain to illustrate a unit step dynamic response corresponding to a change in armature voltage, and the zero positions for each transient are shifted appropriately on the vertical axis. The transient response results for this system indicate very little damping of the load-spring oscillations for large values of  $R_d$ , while smaller values of  $R_d$  lead to a load-motor interaction which quiets the oscillations.

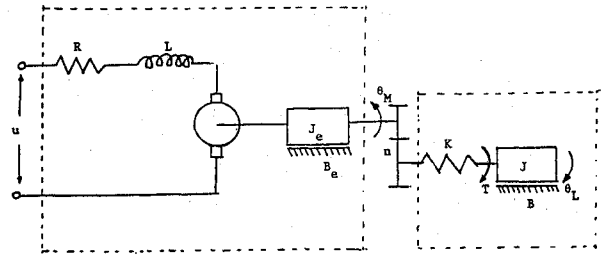


Fig. 1 Armature controlled motor driving a flexible inertial load.

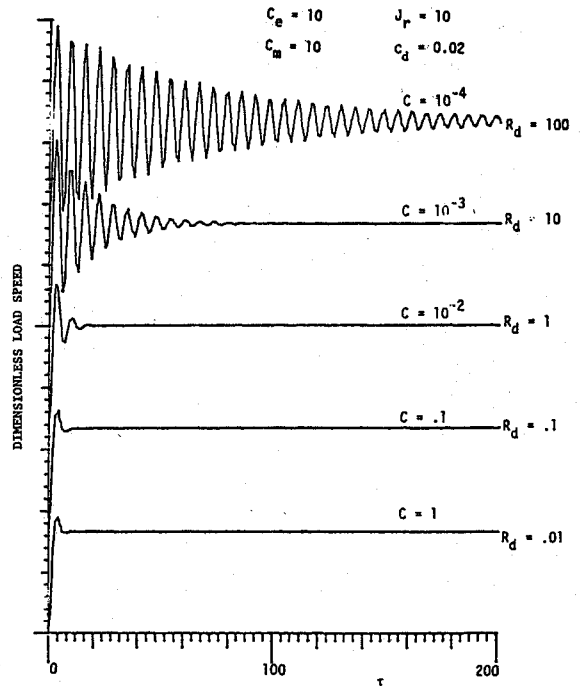


Fig. 2 Typical step response transients (zero positions shifted for clarity, C corresponds to Eq. (9)).

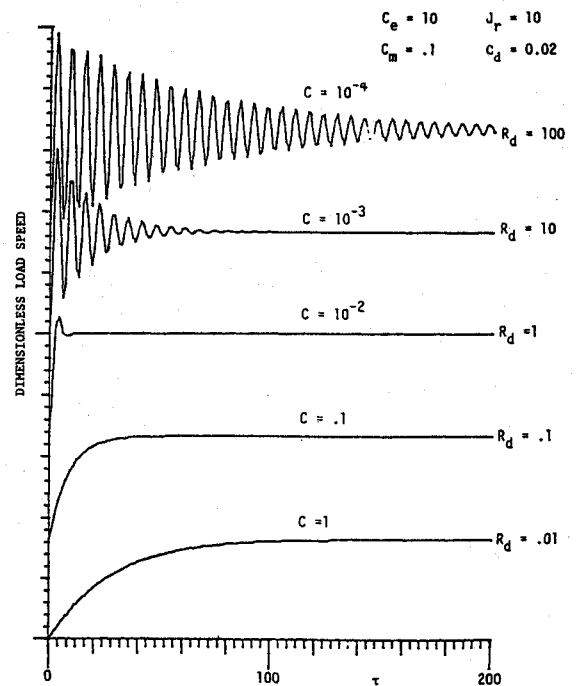


Fig. 3 Step response transients with reduced motor friction effects,  $C_m$ .

The values of  $J_r = 10$  used in Fig. 2 is thought to be a typical ratio of effective load-motor inertias. Small values of  $J_r$  tend to prevent damping of the load oscillations. For example, reducing the relative load inertia in Fig. 2 to  $J_r = 0.1$  results in a very lightly damped oscillatory behavior for all of the step responses shown. The result of reducing the motor mechanical friction parameter to  $C_m = 0.1$  is shown in Fig. 3. The oscillatory system behavior still occurs for large  $R_d$ , while for small  $R_d$ , the slow motor dynamics are now dominant and the load oscillations are not excited. Reducing  $C_e$  has a similar effect. In Fig. 4, transients for  $J_r = 1$  are presented where the smaller values of  $R_d$  show small oscillations superimposed on the slowed motor dynamics. In cases such as this, with oscillations at low values of  $R_d$ , the oscillation frequency results from interaction of the motor and load inertias through the compliant drive and is higher than the load natural frequency itself.

From the various simulation results it has been established that  $J_r$  and  $R_d$  are the two critical parameters in the motor-compliant load interaction. For small values of  $J_r$  (beginning somewhat less than unity), the load interaction with the motor is limited and the motor's motion tends to serve directly as input to the compliant drive shaft producing very oscillatory behavior in the load response. For the larger values of  $J_r$ , the load inertia interacts with the motor dynamics so that the overall system response is influenced more by the motor characteristics. The value of  $R_d$  then takes on particular importance with smaller values of  $R_d$ , allowing the motor resistance to damp the load oscillations. A value of  $R_d$  near unity tends to provide adequate damping without slowing down the system.

In a further effort to select  $R_d$ , a number of numerical optimizations were performed on the open-loop transient response for a step voltage input. The performance criterion considered was in the form of integral-time-absolute-error with the "error" defined as the difference between the load speed and its steady-state value. An initial solution was obtained for a simplified system model neglecting motor inductance, motor inertia and motor friction with  $C_d = 0.02$ . This simplified model leads to a one-dimensional optimization of  $R_d$  and an optimal value of  $R_d = 0.72$ . Similarly, optimizations were performed on the full system model holding  $C_e = 10$ ,  $J_r = 10$  and  $C_d = 0.02$ , while adjusting  $R_d$  and  $C_m$  to minimize the same integral performance index. A number of numerical optimizations from various starting points yielded optimal values of approximately  $R_d = 0.75$  and  $C_m = 0.14$ . These results support the conclusion that a value of  $R_d$  near unity seems to be desirable for good open-loop responses.

### Quantitative Controllability

Since the motor-compliant load system is to be a plant under closed-loop control, its controllability as well as its open-loop behavior, should be of concern in parameter selection. The controllability matrix for the system of Eq. 4 is

$$V = [\bar{G} \quad \bar{F}\bar{G} \quad \bar{F}^2\bar{G} \quad \bar{F}^3\bar{G}]$$

and for the system matrices of Eqs. 7 and 8 this becomes

$$V = \begin{bmatrix} 1 & -C_e & C_e^2 - C_e R_d J_r & -C_e^3 + 2C_e^2 R_d J_r + C_m C_e R_d J_r \\ 0 & C_e R_d J_r & -C_e^2 R_d J_r - C_m C_e R_d J_r & C_e^2 R_d J_r - C_e^2 R_d^2 J_r^2 + C_m C_e^2 R_d J_r + C_m^2 C_e R_d J_r \\ 0 & 0 & C_e R_d J_r & -C_e^2 R_d J_r - C_m C_e R_d J_r \\ 0 & 0 & 0 & C_e R_d J_r \end{bmatrix}$$

The controllability of the system rests on the determinant of  $V$  which equals  $(C_e R_d J_r)^3$ . Thus  $V$  is of full rank, and the system is controllable when  $C_e$ ,  $R_d$  and  $J_r$  are all nonzero. In an effort to quantify the concept of controllability, Friedland<sup>10</sup> proposed a measure of controllability

$$C = |\lambda_{\min}(VV^T)| / |\lambda_{\max}(VV^T)| \quad (9)$$

where  $\lambda_{\min}$  and  $\lambda_{\max}$  represent the smallest and largest eigenvalue magnitudes of the matrix  $VV^T$ . The value of  $C$  ranges from zero for an uncontrollable system to unity where the system is expected to be most controllable. For the  $V$  matrix above, the eigenvalues of interest are  $\lambda_1 = 1$ ,  $\lambda_2 = \lambda_3 = \lambda_4 = C_e R_d J_r$ , and the resulting controllability measure is

$$C = \begin{cases} 1/C_e R_d J_r & \text{for } C_e R_d J_r \geq 1 \\ C_e R_d J_r & \text{for } C_e R_d J_r < 1 \end{cases}$$

Values of  $C$  are shown on the open-loop transient response curves of Figs. 2-4 where it should be noted that low values of the controllability index tend to correspond to oscillatory behavior. However, there is not a one-to-one correspondence between preferred open-loop response and the value of the controllability index  $C$ .

To further explore the nature of the controllability index, its relationship to open-loop system behavior, and its influence on closed-loop system performance, a simplified motor-load system has been considered. Neglecting inductance, inertia and friction in the motor, the system equations become

$$\dot{X} = \begin{bmatrix} 0 & 1 \\ -(1 + C_d R_d^{-1}) & -(C_d + R_d^{-1}) \end{bmatrix} X + \begin{bmatrix} 0 \\ 1 \end{bmatrix} U \quad (10)$$

with state variables of load speed and acceleration. It should be noted that manipulation of Eq. (10) can demonstrate the basic nature of  $R_d$  influence. The damping ratio of the simplified system is defined by the choice of  $R_d$  and the motor resistance serves to dissipate the system energy. From the controllability viewpoint, the matrix

$$V = \begin{bmatrix} 0 & 1 \\ 1 & -(C_d + R_d^{-1}) \end{bmatrix}$$

where the desired eigenvalues are given by

$$\lambda = \frac{-(C_d + R_d^{-1}) \pm [(C_d + R_d^{-1})^2 + 4]^{1/2}}{2} \quad (11)$$

and the maximum controllability index is expected for  $C_d + R_d^{-1} = 0$ . Since  $C_d$  is small, this condition is approached for large values of  $R_d$ , but a large value of  $R_d$  corresponds to a poorly behaved open-loop system and contradicts the  $R_d \approx 1$  conclusion reached in our discussions of the open-loop behavior. To investigate this contradiction, the closed-loop performance of the second order system in Eq. 10 has been considered. The closed-loop characteristic equation is given by

$$\lambda^2 + [(C_d + R_d^{-1}) - k_2]\lambda + [1 + C_d R_d^{-1} - k_1] = 0 \quad (12)$$

where  $k_1$  and  $k_2$  are the feedback gains for load speed and acceleration respectively. A closed-loop system with a natural frequency of ten will be an order of magnitude faster than the open-loop system and with optimal damping in an integral

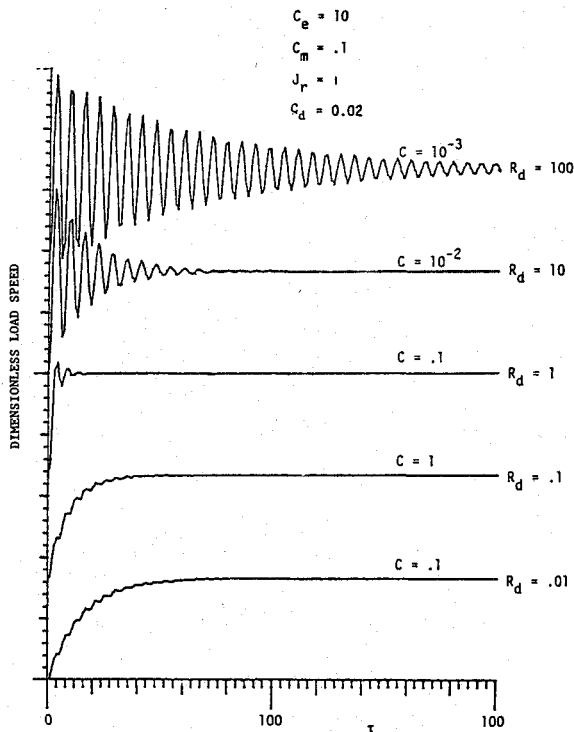


Fig. 4 Transients with reduced  $J_r$  and  $C_m$ .

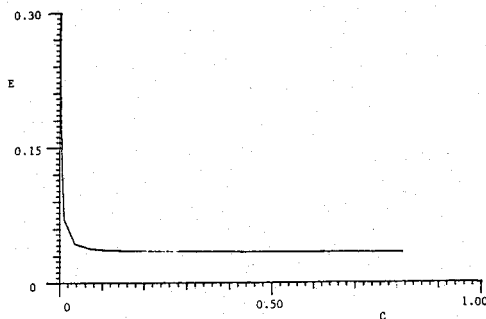


Fig. 5 Control effort vs controllability index.

time absolute error (ITAE) sense,<sup>12</sup> its characteristic equation should be

$$\lambda^2 + 14\lambda + 100 = 0 \tag{13}$$

Equation 12 will take on this form with feedback gains of  $k_1 = -99 + 0.02R_d^{-1}$  and  $k_2 = -13.98 + R_d^{-1}$  for the considered value of  $C_d = 0.02$ . Thus the specified dynamic behavior can be obtained for any reasonable value of  $R_d$  (and controllability index  $C$ ) by adjusting the feedback gains. However, it might be expected that the most "controllable" motor-load system should take the least control effort to achieve the desired dynamic behavior. Numerical simulations were used to compute the control effort for closed-loop systems tuned to satisfy Eq. (13) with various values of  $R_d$ . The measure of control effort was taken as

$$E = \int_0^2 U^2 d\tau \tag{14}$$

and the results for  $E$  are plotted as a function of the controllability index  $C$  in Fig. 5. Clearly the control effort is reduced as  $C$  increases, but an asymptote is approached for  $C$  greater than approximately 0.05. The ideal value of  $C = 1$  need not be reached to have a reasonable level of effort. Figure 6

Table 1 Characteristics of the sample motors

	Motor A	Motor B
Maximum torque, oz-in.	50	2688
Maximum power, W	50	1480
Armature resistance, $\Omega$	3.9	8.6
Armature inductance, H	0.0023	0.0258
Back EMF, V/rad/sec	0.1	0.89
Motor constant, oz-in./A	13.9	125.0
Motor friction, oz-in-sec	0.36	13.7
Motor inertia, oz-in-sec <sup>2</sup>	0.0026	0.4

Table 2 Values of the dimensionless parameters

	$J_r \approx 1$		$R_d \approx 1$	
	Motor A	Motor B	Motor A	Motor B
$C_e$	170	33	170	33
$C_m$	14	3.4	14	3.4
$R_d$	20	3.2	1	1
$J_r$	0.7	1	11.1	3.3
$C_d$	0.02	0.02	0.02	0.02
Gear ratio, $n$	0.01	0.15	0.04	0.27
Control index, $C$	0.0004	0.01	0.0004	0.01

shows the index  $C$  vs  $R_d$  and is also asymptotic, with  $C$  near unity for larger values of  $R_d$ . The values of  $R_d$  near unity which give preferred damping and open-loop behavior for this system correspond to  $C$  of about 0.4 and, accordingly, have a very respectable closed-loop control effort.

### Closed-Loop Control of a Specified Load

In order to evaluate the concepts presented in the previous sections, a series of examples have been solved based on the linear model of Fig. 1 and the full set of Eqs. (1-3). These examples consider a given load with an inertia  $J = 18$  oz in. s<sup>2</sup>, a drive compliance which yields a natural frequency  $\sqrt{K/J} = 10$  rad/s, and an assumed damping ratio of  $C_d = 0.02$ . Two servo motors have been selected from a manufacturer's catalog (Magnetic Technology, Canoga Park, CA), and the parameters for each are shown in Table 1. Note that motor A is relatively small and motor B is relatively large. Linear state variable feedback has been considered for control of the system of Eqs. 1-3, and the resulting closed-loop behavior has been tailored to yield a specified step response transient in the load speed  $x_4 - \theta_L$ . Optimal control concepts have been used in the design of the control loop, and the influence of motor choice and gear ratio on the performance of the resulting controllers is discussed below.

The first choice of gear ratio is based on the popular notion of matching effective load and motor inertias. This has been recommended<sup>13</sup> to minimize armature energy dissipation and, in our dimensionless notation, corresponds to keeping  $J_r$  near unity. Gear ratios of  $n = 0.01$  and 0.15 have been selected on this basis for motors A and B, and the resulting values for the dimensionless parameters and the controllability measure  $C$  are shown in Table 2. The gear ratios have also been chosen based on our earlier conclusions that  $R_d$  near unity is desired to have good open-loop response of the motor-load system. This requires

$$n = [K_M K_g / R J \sqrt{K/J}]^{1/2}$$

and leads to values of  $n = 0.04$  and 0.27 for the two motors as indicated in Table 2. The controllability measure  $C$  is gear ratio independent, and the value for motor B ( $C = 0.01$ ) is better than for motor A ( $C = 0.0004$ ).

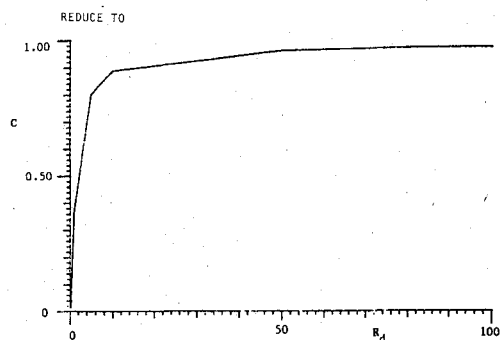


Fig. 6 Controllability index C vs motor parameter  $R_d$ .

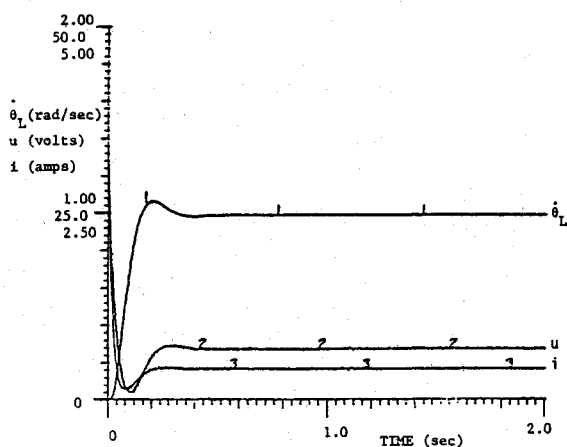


Fig. 7 Motor B closed-loop response for  $R_d = 1$ .

With linear state variable feedback the system input  $u = K^T x$  where  $K = [k_1 k_2 k_3 k_4]^T$  represents the feedback gains. These gains have been selected by solving the infinite time optimal control problem<sup>14</sup> using the performance index

$$J = \int_0^{\infty} [x^T Q x + R u^2] dt \quad (15)$$

where  $Q$  has been considered as a diagonal matrix with positive entries and  $R$  as a positive scalar. The matrix Riccati equations were solved by integrating backwards in time. The goal of the optimal control performance was to achieve a well damped step response transient in load speed with a settling time of approximately 0.3 s. The desired transient response yielding a load speed  $\dot{\theta}_L = 1$  rad/s is shown by curve 1 in Fig. 7. For each of the four cases in Table 2, the values of the weighting factors  $Q$  and  $R$  in Eq. (15) were adjusted so that the desired transient in  $\dot{\theta}_L$  was duplicated. This adjustment was performed via an interactive graphics computer program which permitted rapid review of transient responses and corresponding tuning of the weighting factors for the optimal controllers. In each case, the reference input to the control loop was adjusted as necessary to allow viewing the transient response to a steady load speed of 1 rad/s.

The sample step response curves shown in Fig. 7 are the final results obtained for the control of motor B with a gear ratio corresponding to  $R_d = 1$ . The transient responses for the final optimal control designs of the other systems in Table 2 show identical  $\dot{\theta}_L$  transients, and the curves for  $u(t)$  and  $i(t)$  have the same general form. However, the overall control effort for the four cases differs substantially as summarized in Table 3. Here it is seen, despite the attempt to minimize control effort in each case, that both motors require considerably less input with  $R_d = 1$ . The peak voltage, peak current and

Table 3 Control results for the two sample motors

	$J_r \approx 1$		$R_d \approx 1$	
	Motor A	Motor B	Motor A	Motor B
Maximum $u$ , V	100	59	25	32
Maximum $i$ , A	20.1	5.2	5.1	2.8
Maximum power, W	2000	300	130	88
Dissipation <sup>a</sup> $E$ , J	55.5	12.2	3.73	3.6

<sup>a</sup>Based on resistive losses in first two seconds.

peak power inputs are all reduced as well as the overall energy dissipated during the transient. On both sides of Table 3, motor B shows less required effort than motor A. This apparently reflects the higher level of controllability index  $C$  previously noted.

Of course, there are many other practical bases for selecting a motor than those mentioned above. The purpose of this study has been only to evaluate the linear performance of the motor-load system, and any nonlinear aspects of the system response (including saturation) have been neglected in the results presented. However, the final result for our realistic example does show best performance corresponding to  $R_d = 1$  and the highest value of the controllability index.

### Conclusions

This paper has described the behavior of a DC servomotor actuating a lightly damped compliant load. Parameter values are identified which permit open-loop system damping by electromechanical interaction. Also Friedland's controllability index has been defined for the system. Closed-loop control of load speed was considered for specific cases, and, with time response requirements, reduced control effort was needed in systems selected for good open-loop behavior. However, best control corresponded to good open-loop behavior and a higher value of the controllability index.

Results of this effort indicate potential benefits for the integrated design of motor-load control systems particularly with compliant loads. Control of such systems should be enhanced by careful selection of a motor to match its load in a dynamic sense. In fact, overall optimization of a control, motor and load system may well be appropriate to parametrically optimize a plant while considering its performance within a control loop. This study of motor-load interaction has been confined to a simple lumped parameter model; however, it seems appropriate to extend this effort to explore motor-load interactions for distributed parameter systems frequently of interest in robotics and space structures.

### References

- Dubowsky, S., and Desforges, T.D., "The Application of Model-Referenced Adaptive Control to Robotic Manipulators," *Journal of Dynamic Systems, Measurement and Control*, Vol. 101, No. 3, 1979, pp. 193-200.
- Lul, S.Y.S., Fisher, D.F., and Paul, R.P., "Joint Torque Control by a Direct Feedback for Industrial Robots," *IEEE Transactions, Automatic Control*, Vol. AC-28, 1983, pp. 153-161.
- Franklin, F.G., and Powell, J.D., *Digital Control of Dynamic Systems*, Addison-Wesley, 1980.
- Dombre, E., Liegeois A., and Borrel, P., "Modelling the Elastic Transmissions of a Computer Controlled Manipulator," *IEEE Conference on Decision and Control*, 1980.
- Yamada, I., and Nakagawa, M., "Reduction of Residual Vibrations in Positioning Control Mechanisms," *ASME Transactions, Journal of Vibrations, Acoustics, Stress and Reliability in Design*, Vol. 107, No. 1, 1985, pp. 47-52.
- Sturm, J.A., Erdman, A.G., and Wang, S.-H., "Design and Analysis of an Industrial (3P3R) Robot," *ASME Design Engineering Technical Conference*, ASME Paper 82-DET-39, Washington, 1982.

<sup>7</sup>Meckl, P., and Seering, W., "Active Damping in a Three-Axis Robotic Manipulator," *ASME Transactions Journal of Vibrations, Acoustics, Stress and Reliability in Design*, Vol. 107, No. 1, 1985, pp. 38-46.

<sup>8</sup>Paul, R.P., *Robot Manipulators: Mathematics, Programming and Control*, The MIT Press, Cambridge, MA, 1981.

<sup>9</sup>Wagle, M.M., "Control of a Motor-Load System with Light Mechanical Damping," M.S. Thesis, State University of New York at Buffalo, 1981.

<sup>10</sup>Friedland, B., "Controllability Index Based on Conditioning Number," *Journal of Dynamic Systems, Measurement and Control*, Dec. 1975, pp. 444-445.

<sup>11</sup>Harokopos, E.G., "Control of a Flexible Servomechanism," MS Thesis, Mechanical Engineering, State University of New York at Buffalo, 1983.

<sup>12</sup>Ogata, K., *Modern Control Engineering*, Prentice-Hall, New York, 1970.

<sup>13</sup>*DC Motors, Speed Controls, Servo Systems: An Engineering Handbook*, Electro-Craft Corp., Hopkins, MN, Fifth Edition, 1980.

<sup>14</sup>Anderson, B., and Moore, J.B., *Linear Optimal Control*, Prentice Hall, New York, 1971.

*From the AIAA Progress in Astronautics and Aeronautics Series...*

## AERODYNAMIC HEATING AND THERMAL PROTECTION SYSTEMS—v. 59 HEAT TRANSFER AND THERMAL CONTROL SYSTEMS—v. 60

*Edited by Leroy S. Fletcher, University of Virginia*

The science and technology of heat transfer constitute an established and well-formed discipline. Although one would expect relatively little change in the heat-transfer field in view of its apparent maturity, it so happens that new developments are taking place rapidly in certain branches of heat transfer as a result of the demands of rocket and spacecraft design. The established "textbook" theories of radiation, convection, and conduction simply do not encompass the understanding required to deal with the advanced problems raised by rocket and spacecraft conditions. Moreover, research engineers concerned with such problems have discovered that it is necessary to clarify some fundamental processes in the physics of matter and radiation before acceptable technological solutions can be produced. As a result, these advanced topics in heat transfer have been given a new name in order to characterize both the fundamental science involved and the quantitative nature of the investigation. The name is Thermophysics. Any heat-transfer engineer who wishes to be able to cope with advanced problems in heat transfer, in radiation, in convection, or in conduction, whether for spacecraft design or for any other technical purpose, must acquire some knowledge of this new field.

Volume 59 and Volume 60 of the Series offer a coordinated series of original papers representing some of the latest developments in the field. In Volume 59, the topics covered are 1) the aerothermal environment, particularly aerodynamic heating combined with radiation exchange and chemical reaction; 2) plume radiation, with special reference to the emissions characteristic of the jet components; and 3) thermal protection systems, especially for intense heating conditions. Volume 60 is concerned with: 1) heat pipes, a widely used but rather intricate means for internal temperature control; 2) heat transfer, especially in complex situations; and 3) thermal control systems, a description of sophisticated systems designed to control the flow of heat within a vehicle so as to maintain a specified temperature environment.

*Published in 1976*

*Volume 59—424pp., 6×9, illus., \$25.00 Mem., \$45.00 List*  
*Volume 60—382 pp., 6×9, illus., \$25.00 Mem., \$45.00 List*

TO ORDER WRITE: Publications Dept., AIAA, 1633 Broadway, New York, N.Y. 10019